Journal of Chemical Technology and Metallurgy, 58, 1, 2023, 53-67

ONE STEP COMPARATIVE STUDY BY HIRSHFELD SURFACE ANALYSIS, ENERGY FRAMEWORKS AND DFT OF HYBRID ORGANIC-INORGANIC PHOSPHATE

Abdellatif Rafik[1] , Hafid Zouihri[2] , Taoufiq Guedira[1]

[1]Laboratory of Organic Chemistry, Catalysis and Environment
Faculty of Sciences, Ibn Tofail University, B.P. 133, 14000
Kenitra, Morocco
[2]Laboratory of Chemistry of Materials and Biotechnology of Natural Products
University Moulay Ismail, Faculty of Sciences
Meknes, Morocco
E-mail: abdellatif.rafik@uit.ac.ma

Received 04 April 2022
Accepted 10 June 2022

ABSTRACT

The crystal packing of the title compound is stabilized by intra and intermolecular O–H···N and C–H···O hydrogen bonds. This system of hydrogen bonds involves two neighboring molecules in the same plane. The geometric parameters of 3-acetylanilinium dihydrogen phosphate [3-2ADP] compound in ground state, calculated by density functional theory (B3LYP) and Hartree-Fock (HF) methods with the 3-21G basis set, are in good agreement with the X-ray study, because of the geometry of the crystal structure is subject to intermolecular forces, such as van der Waals interactions and crystal packing forces, while only intramolecular interactions were considered for isolated molecule. The energy gap was found using HOMO and LUMO calculations, the less band gap indicates an eventual charge transfer within the molecule.

Keywords: Hartree-Fock, Dos, hydrogen bonding, HOMO, LUMO, Hirschfeld surfaces.

INTRODUCTION

Organic-inorganic crystals typically have attractive characteristics of nonlinear optical behavior. However, their mechanical and thermal properties for devices are inadequate. In comparison, inorganic crystals have the higher mechanical properties and thermal stability. Their optical nonlinearity in nature is mild [1 - 3]. Combined organic and inorganic properties shall be shared by the semi-organic class of materials produced by combining inorganic acid and organic ligand. Due to the flexibility of these structures, organic-inorganic hybrid materials received considerable attention, which gives a rich and fertile playground for the elaboration of interesting crystal structure with different physical properties. Furthermore, there are many interesting aspects of inorganic and organic phosphate chemistry. These hybrids and their derivatives received considerable attention due to their interesting dielectric properties [4], optoelectronic [5], etc. It should be noted that phosphate and its derivatives are in commercial use more than any other elements. Considering the attractive properties of phosphate and the new promising opportunities that may open with regard to the development of useful organic-inorganic hybrid materials, we report in this work a combined experimental and a theoretical studies of a new hybrid compound namely, 3-acetylanilinium dihydrogen phosphate [6]. The crystal structure was determined by single crystal X-ray diffraction [7].

The hybrid of 3-acetylanilinium dihydrogen phosphate is an interesting nonlinear optical material, whose molecular derivatives are corresponding to the aniline. It is an organic and inorganic compound, its derivatives undergo strong hydrogen bond (N-H) interactions and this characteristic could serve as a significant function of supramolecular chemistry due to their interesting physical and chemical properties [8 - 10]. Inorganic phosphate-based salts were also typical in nonlinear optical applications due to their inherent ionic character and spheroidal structure with a broad delocalized π-electron system [11 - 13]. Moreover, DFT calculations reveal the good correlation between crystal structure and physical properties. Hirschfield surface analysis and molecular electrostatic potential (MEP) were also calculated. Here we report for the first time the structural characterization of 3-2ADP molecule by X-ray diffraction analysis and the results of our calculations using density functional theory (B3LYP) and Hartree-Fock (HF) methods with the 3-21G basis set, which are chosen to study the structural, geometric and charge transfer properties of 3-2ADP molecule in the ground state. In this paper, the results of the characterization are discussed in detailed.

EXPERIMENTAL

Hirschfeld surface method

The Hirshfeld surfaces and the associated 2D fingerprint plots were calculated using the Crystal Explorer program, which accepts a structure input file. A Hirshfeld surface is the outer contour of the space, which a molecule or an atom consumes in a crystalline environment [14]. The normalized contact distance d_{norm} based on both d_e (distance from the point to the nearest nucleus external to the surface) and d_i (distance to the nearest nucleus internal to the surface) and the van der Waals (vdW) radii of the atom, given by equation (1), enables identification of the regions of particular importance to intermolecular interactions[15, 16]:

$$d_{norm} = \frac{(d_i - r_i^{vdw})}{r_i^{vdw}} + \frac{(d_e - r_e^{vdw})}{r_e^{vdw}}$$

The value of the d_{norm} is negative or positive when intermolecular contacts are shorter or longer than vdW separations, respectively. Due to the d_e and d_i symmetry in the d_{norm} expression, where two Hirshfeld surfaces touch, both show a red spot that is similar in colour, size and shape. Using a red – blue – white color scheme the d_{norm} values are mapped to the Hirshfeld surface: red regions correspond to closer contacts and negative d_{norm} value, the blue regions correspond to the longer contacts and the positive d_{norm} value and the white regions are those where the contact distance is precisely the vdW separation and the d_{norm} value is zero.

Computational details

The full geometrical optimization of structure 3-2ADP, especially those using hybrid functional, have evolved to a powerful and very reliable tool, being commonly used for the determination of various properties of molecules. Within the framework of the DFT approach [17], the B3LYP hybrid functional [18], has often been preferred since it is proved efficient in reproducing various molecular properties and the combined use of HF with 3-21G basis set has previously been shown to provide an excellent compromise between accuracy and computational efficiency of selected bond lengths for the 3-2ADP molecule implemented with Gaussian 03 program [19]. The computed geometric parameters of the title compound are reported and compared with the experimental parameters in Table 4.

RESULTS AND DISCUSSION

Crystal structure description

The single crystal X-ray analysis of 3-2ADP revealed that this compound crystallizes in the monoclinic crystal system in the P21/c space group with Z = 4. The asymmetric unit contains one 3-acetylanilinium cation and one dihydrogen phosphate anion (1:1 ratio of cationic to anionic units). The ORTEP view of compound 3-2ADP is shown in Fig. 1. The phosphorous atom of the cation exhibit a slightly distorted tetrahedral geometry, with the bond angles around the P atoms in the range from 107.0(1)$^\circ$ to112.1(1)$^\circ$. The 3D supramolecular network of this compound is dominated by the variety of O-H…O hydrogen bonds. In addition, N-H…O interactions, which can play a crucial role in the stabilization of supramolecular assemblies, the phosphate anions each formed eight O-H...O hydrogen bonds (Fig. 2).

Hirshfeld surface analysis

Hirshfeld surface analysis is used to find out the various intermolecular non-covalent interactions in the crystal system 3-2ADP and it was analyzed using CrystalExplorer 17 package. Two dimensional fingerprint plots and three dimensional Hirshfeld surfaces are shown in Fig. 3. The greater proportion of O-H/H-O contacts is found to be 45.6 % and it is due to the stronger N-H…O and weaker C-H…O intermolecular contacts. Two sharp spikes in 2D fingerprint plot of 3-2ADP reveals that the title compound is strongly stabilized by O/H (N-H…O/C-H…O) interactions. The H…H contacts appear in the center of the 2D fingerprint maps with a broad peak

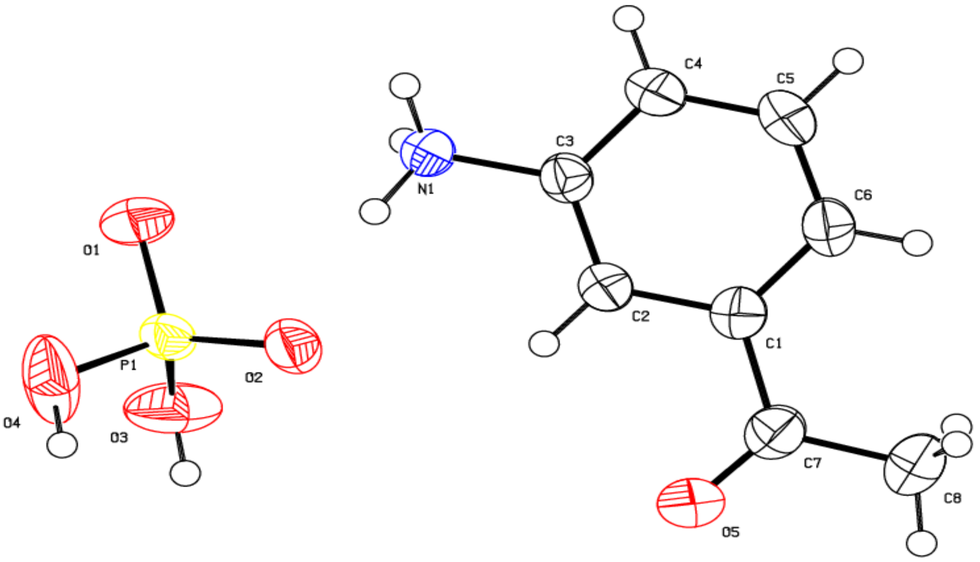

Fig.1. ORTEP diagram with thermal ellipsoids drawn at 50 % probability.

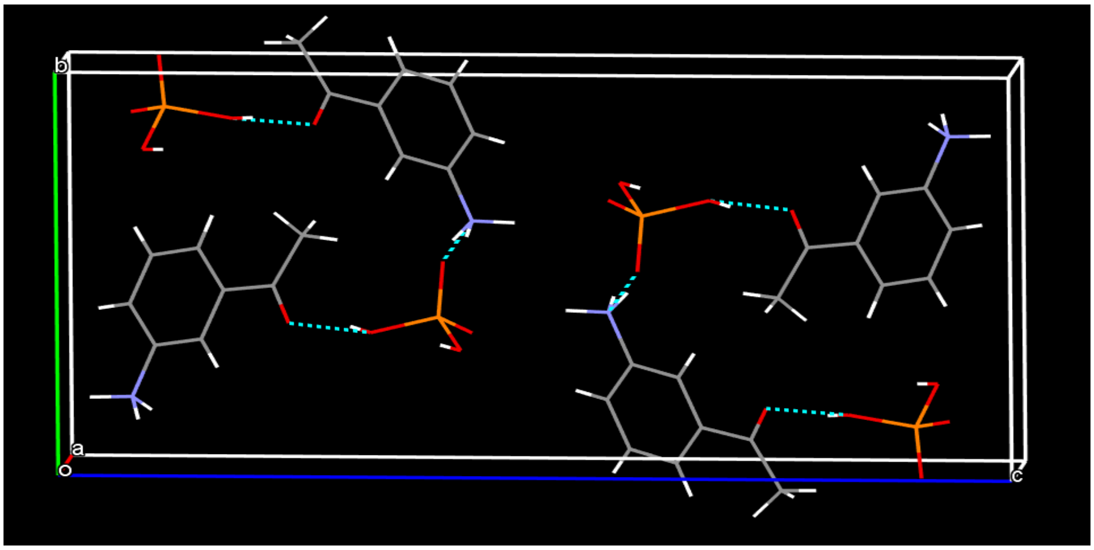

Fig. 2. A view of packing of 3-2ADP with O—H···N hydrogen bond interactions.

at de =di =1.1 Å and with the percentage contribution of 34.8 %. The 10.1 % contribution from C…H/ H…C contacts to the Hirshfeld surface is seen as a pair of wings in 2D fingerprint map. The dark red spot on phosphate oxygen exhibits the electron rich character which enables the intermolecular contacts with neighbor. Shape index clearly explains the availability of inverted bow and tie triangles. It is due to the stronger $\pi \dots \pi$ stacking interactions (Fig. 4). The flat surfaces of curvedness in 3-2ADP establish the availability of ring delocalization and stronger $\pi \dots \pi$ stacking profiles. From the detailed study of 3-2ADP using Hirshfeld surface analysis, it is clear that the compound is stabilized and connected through enormous amount of O…H and appreciable

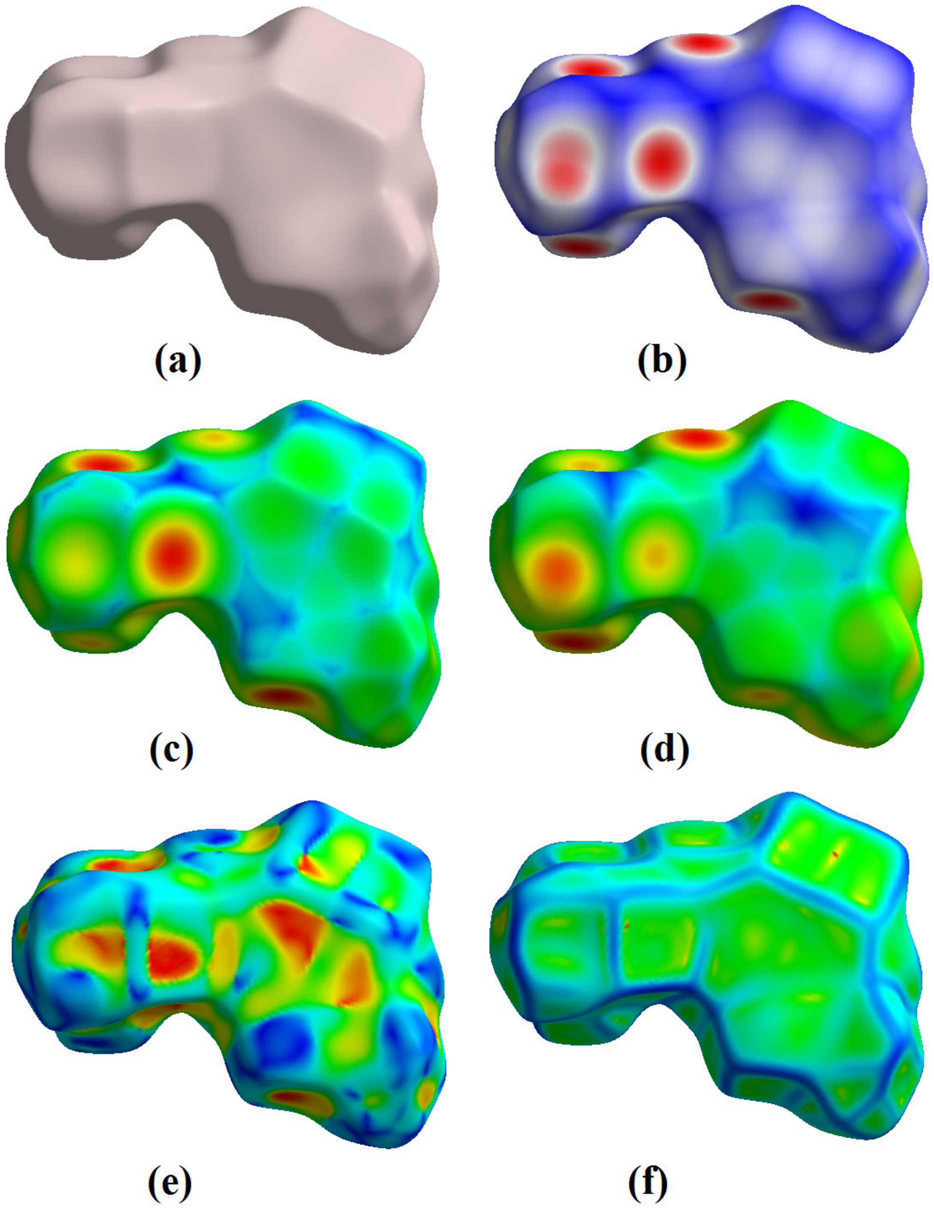

Fig. 3. Hirshfeld surfaces of the molecule of 3-2ADP: (b) d_{norm}, (c) d_e, (d) d_i, (e) Shape index and (f) Curvedness.

level of π... π stacking which enables the optical properties, have very little influence on the molecular packing due to their interatomic distances being equal to or greater than the sum of their van der Waals radii.

The view of the electrostatic potential obtained using CrystalExplorer17 allows the visualization of donors and acceptors of intermolecular interactions in blue and red regions around the participating atoms corresponding to the positive and negative electrostatic potential on the surface, respectively [20]. The view of the electrostatic potential in the range -0,835 to 1,061 a.u., calculated for the title compound at the HF/3-21G level. The acceptors for N—H…O and O—H…O hydrogen bonds are shown as red areas around the O_2 atom related with negative electrostatic potentials as shown in Fig. 5.

Fig. 6 shows the voids in the crystal structure of 3-2ADP. Those are based on the calculation of the densities of the spherical atomic electron at the acceptable nuclear level. The calculation of crystal voids (results below 0.002 a.u. isovalue) shows the vacuum volume of title compound of the order of 116,20 Å^3 and surface area of the order of 434,42 Å^2. The measured

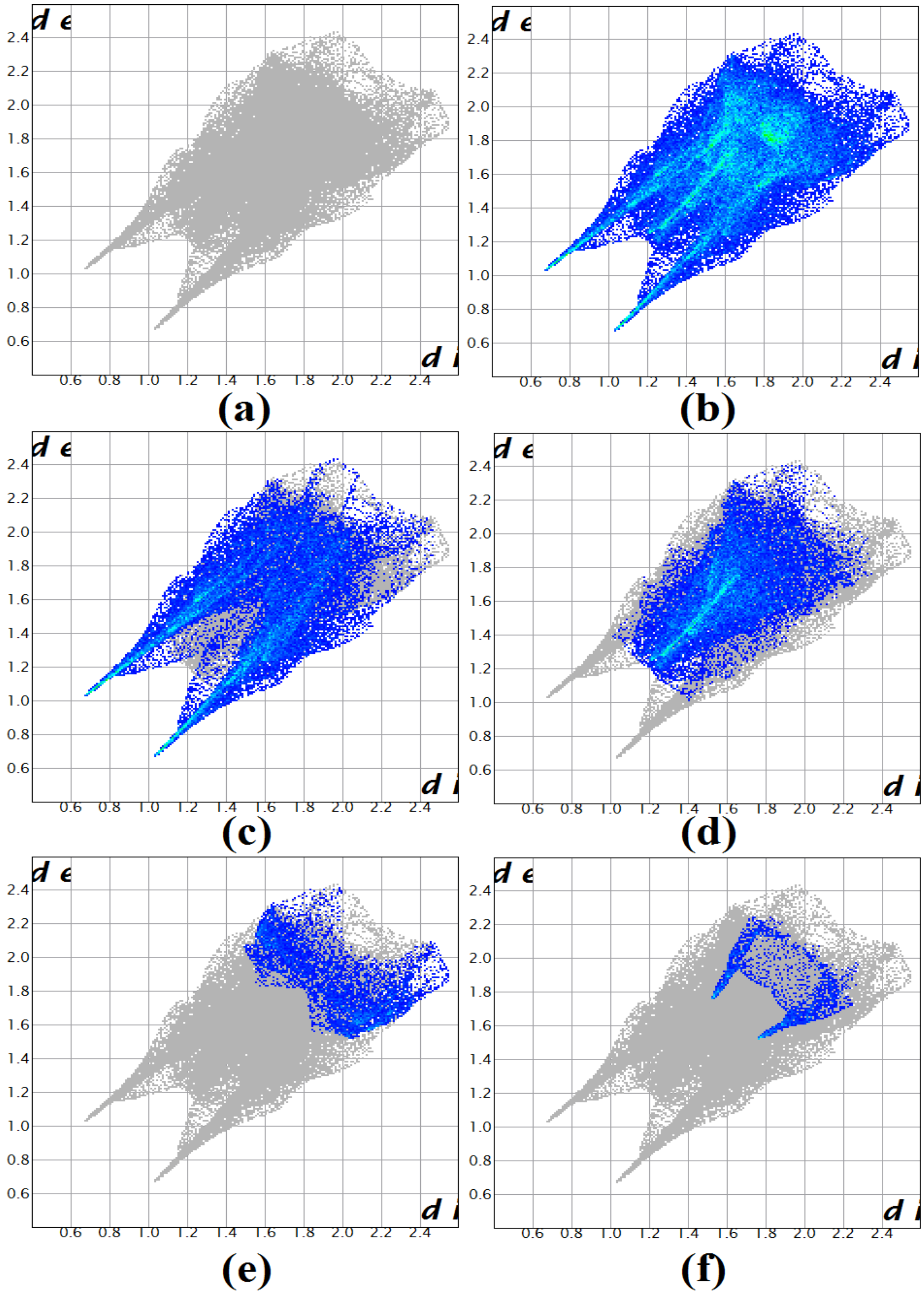

Fig. 4. The full two-dimensional fingerprint plots for the title compound (a), showing (b) all interactions and delineated into (c) O…H/H…O, (d) H…H, (e) H…C/C…H and (f) O…C/C…O, interactions on the Hirshfeld surface contacts.

volume of void of 3-2ADP is 11.10 % with porosity. The cavities are not large. It was noted that the isosurfaces of the electron-density are not fully closed around the elements, but are open at certain positions where, for example, interspecies approaches are found N-H…H.

The supra-molecular architectures for the crystal structures of 3-2ADP were visualized by energy framework calculations, that were performed using CE-B3LYP energy model for a (2x2x2) 3-2ADP block of unit cells (Fig. 7) [20]. Energies between molecular pairs

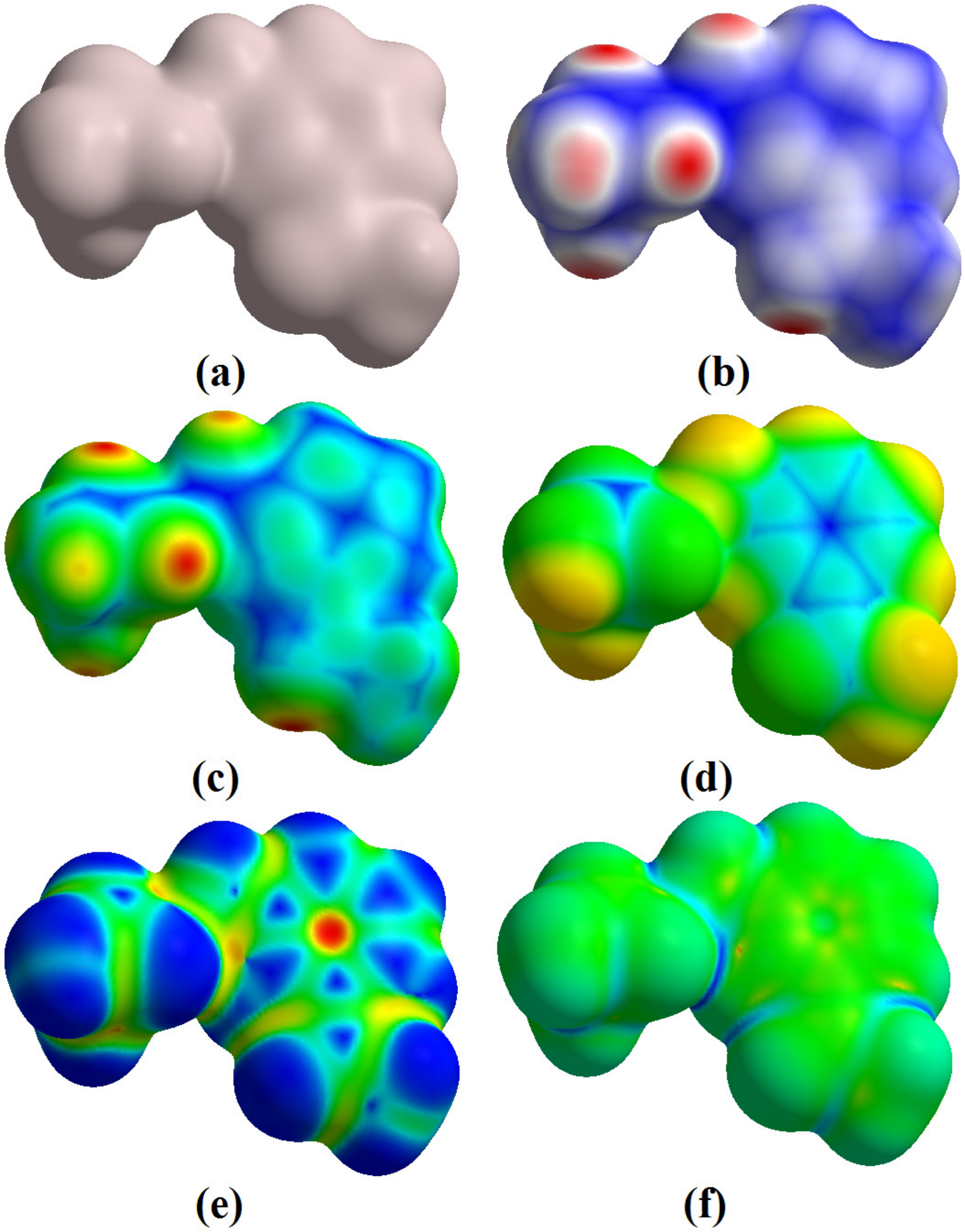

Fig. 5. Electrostatic Potential (PE) mapped on Hirshfeld surface of the molecule of 3-2ADP: (b) d_{norm}, (c) d_e, (d) d_i, (e) Shape index and (f) Curvedness.

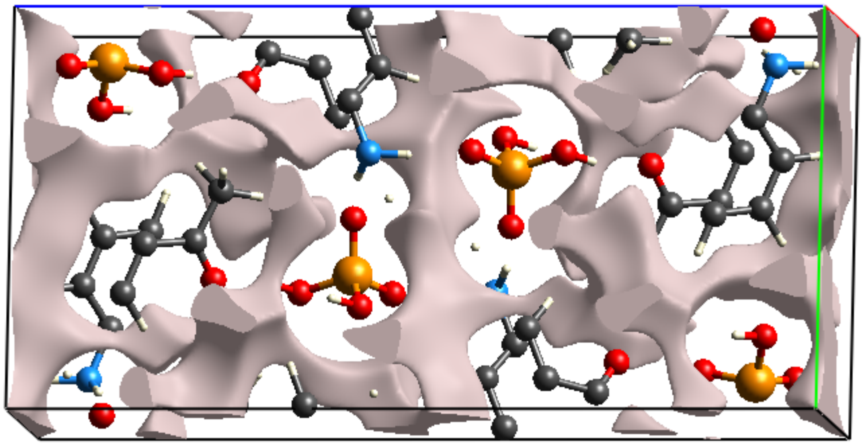

Fig. 6. Crystal Voids of 3-2ADP at 0.002 au isosurface.

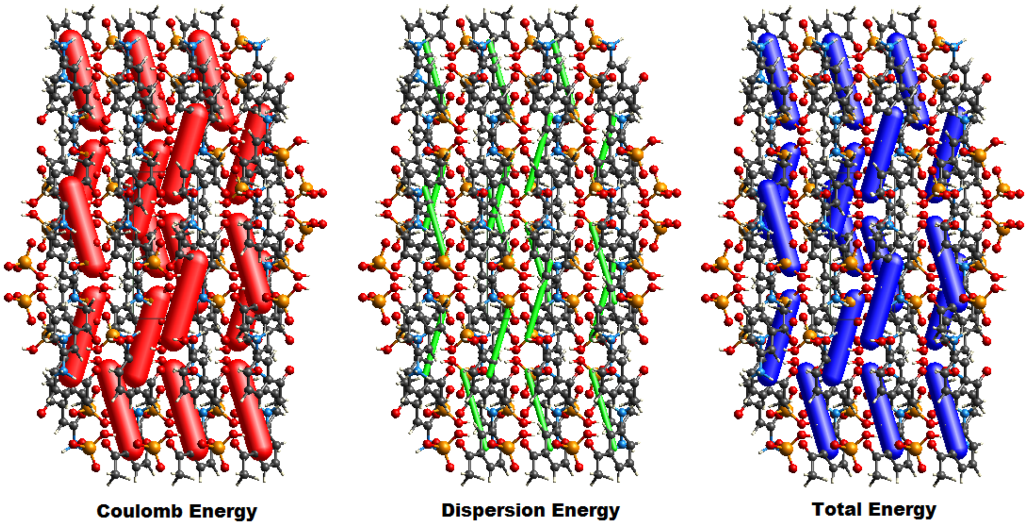

Coulomb Energy **Dispersion Energy** **Total Energy**

Fig. 7. Energy frameworks of 3-2ADP, representing electrostatic, dispersion and total interaction energy terms.

Table 1. Scale factors for benchmarked energy models.

R	Electron Density	$E_{—ele}$	$E_{—pol}$	$E_{—dis}$	$E_{—rep}$	$E_{—tot}$
5.50	B3LYP/6-31G(d,p)	-44.3	-16.9	-13.8	52.6	-38.9

Table 2. Interaction energies (kJ/mol) of the molecular pairs calculated from energy framework calculation of 3-2ADP.

Energy Model	$k_{—ele}$	$k_{—pol}$	$k_{—dis}$	$k_{—rep}$
CE-HF…HF/3-21G electron densities	1.019	0.651	0.901	0.811
CE-B3LYP…B3LYP/6-31G (d.p) electron densities	1.057	0.740	0.871	0.618

are described as cylinders which join the centroids of molecular pairs. Energies between molecular pairs are described as cylinders that join molecular pair centroids. Frameworks were constructed for $E\text{-}_{ele}$ (red cylinders), $E\text{-}_{dis}$ (green) and $E\text{-}_{tot}$ (blue), the scale for tube/cylinder size is 200 and cutoff of 10.00 KJ/mol was used is showing in Tables 1 and 2, respectively.

Geometry optimization

The crystal geometry of 3-2ADP has been determined by DFT and HF methods with 3-21G basis set using the Gaussian 03 program, and was compared with experimentally observed geometrical parameters. The chosen parameter of crystal geometry is shown in Table 3 and optimized molecular structure is shown in Fig. 8. Based on the crystal geometry, the bond length of O_8–C_{20} has been calculated as 1.2520 Å. The bond length between carbon and one oxygen atom was identical which confirm the structure of C=O group and the predominance of vibrancy in carboxylate anion. These dissimilarities of bond distance between C=O at the acetyl portion shows that different environmental oxygen atoms have been bonded with carbon atoms. The bond distance of C–O 1.2240 Å at HF method and 1.2520 Å at DFT method) and bond angles of O–C–C [121.0163° at HF method and 120.4751° at DFT method] of amino fragment implies a deprotonated NH_3^+ group. The values of nitrogen involving dihedral angles such as D (25, 9, 13, and 14) and O_{26}–C_{29}–C_{30}–N_{32} were found to be 24.8305° and -17.4832° at DFT method respectively; This means that the amino band with the acetyl group is planar oriented. It was exactly coincided with the experimental (Table 3).

Table 3. Comparison of selected bond lengths [Å] for 3-2ADP crystal.

Bond lengths	Experimental	HF/3-21G	DFT/B3LYP/3-21G
R(1,2)	1.50	1.54	1.57
R(1,3)	1.49	1.62	1.66
R(1,4)	1.56	1.60	1.63
R(1,6)	1.54	1.61	1.66
R(3,27)	1.92	0.98	1.03
R(4,5)	0.81	0.98	1.02
R(6,7)	0.81	0.96	0.99
R(8,20)	1.21	1.22	1.25
R(9,13)	1.45	1.40	1.41
R(9,25)	0.96	1.00	1.01
R(9,26)	0.91	1.01	1.04
R(9,27)	0.96	1.98	1.78
R(10,11)	1.40	1.37	1.39
R(10,18)	1.39	1.38	1.40
R(10,20)	1.48	1.48	1.48
R(11,12)	0.93	1.06	1.08
R(11,13)	1.37	1.38	1.39
R(13,14)	1.38	1.38	1.40
R(14,15)	0.92	1.07	1.08
R(14,16)	1.38	1.38	1.39
R(16,17)	0.93	1.07	1.08
R(16,18)	1.38	1.38	1.39
R(18,19)	0.92	1.07	1.08
R(20,21)	1.48	1.50	1.51
R(21,22)	0.96	1.07	1.09
R(21,23)	0.96	1.08	1.09
R(21,24)	0.95	1.08	1.09

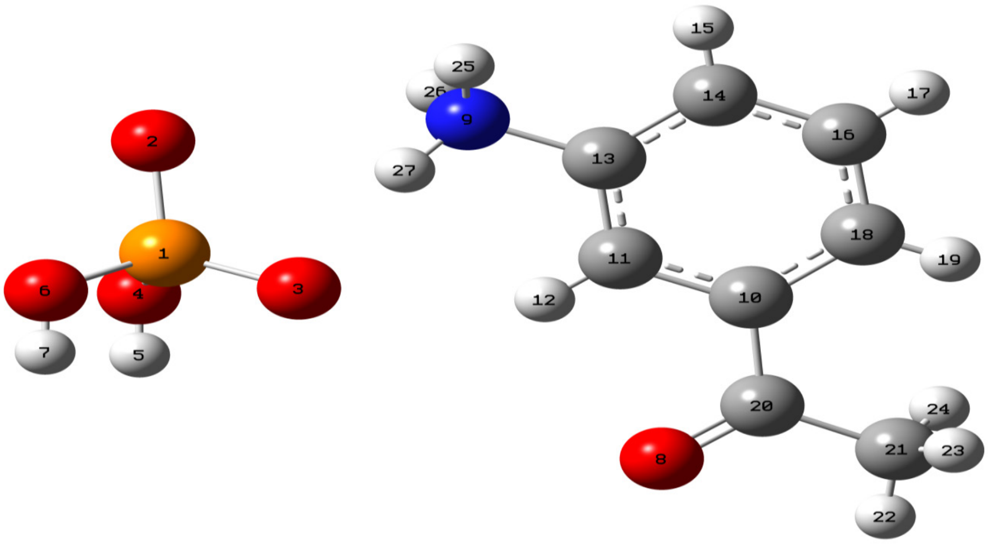

Fig. 8. Optimized molecular structure of 3-2ADP calculated at DFT level.

HOMO-LUMO analysis and DOS

To obtain details about the composition of the molecular orbital (MO), the energies of the 3-2ADP molecule HOMO (π-donor) and LUMO (π-acceptor) are examined via the B3LYP level at the value of 6-31G. The expansion of the word HOMO is the molecular orbital with highest occupation. Orbital of HOMO and LUMO are displayed in Fig. 9. HOMO and LUMO energies and their band gap energy exhibit the actual molecular chemical reaction. Naturally, HOMO is called as an electron donor due to having the capability to contribute an electron. LUMO is called as an electron acceptor due to having the capacity to grab an electron (Fig. 9). The energies of HOMO and LUMO are reckoned at -0. 23 a.u. and -0.07 a.u., correspondingly. As 4.23 eV the band difference between HOMO and LUMO is noted. HOMO and LUMO computed energies have shown that the transfer of charge is taking place within the molecule itself. The low energy gap value declares the appropriateness of the 3-2ADP grown in NLO field [21]. Some important quantum chemical parameters such as ionization potential (I), electron affinity (A), electronegativity (χ), chemical potential (μ), chemical hardness (η), chemical softness (S) and electrophilicity index(ϖ) were calculated theoretically by using the energy values of frontier molecular orbitals [22-25] and the results are presented in Table 4.

The contributions of molecular orbitals and the density of states of 3-2ADP molecules are calculated from Gauss-Sum program and are shown in Fig. 10. The HOMO and LUMO levels are indicated from DOS spectrum as green and red lines, respectively. The DOS spectrums were used to initiate determination of the energy difference between HOMO and LUMO. Through this study, the molecule can be graded as a hard and soft molecule for the small and wide energy differences, respectively. Using the molecular electrostatic potential (MEP) diagram, the probability of electrophilic and nucleophilic reactions and other charging-related properties is observed to visualize the charging distribution of molecules.

Energy gap between HOMO and LUMO is a vital stricture in determining molecular electrical transport properties [26]. Orbitals significantly overlap near phosphate atom and charge transfer occurs through amino group. Group contributions of molecular orbital spectra to prepare state density (DOS), PDOS and COOP (crystal orbital overlap population) are mapped using the Gauss-Sum program as in the Fig. 10 [27 - 32]. Contributions to chemical bonding via PDOS plots show a group percentage contribution to each molecular orbital. Positive value of COOP indicates bonding interaction, negative value indicates anti bonding interaction and zero value indicates nonbonding interactions. COOP diagram reveals that 3-acetylanilinium ring have strong bonding and anti-bonding characters, the gap energy 4.23 eV it is presents attractive physical properties to be used as a substrate for the fabrication of detectors.

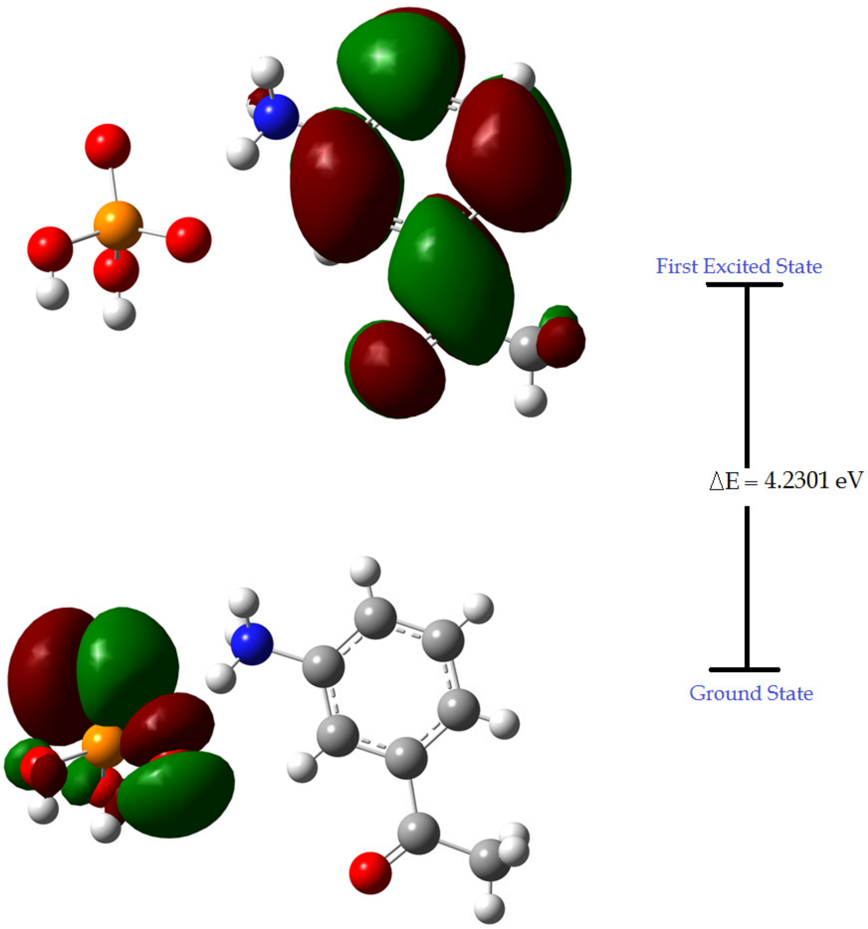

Fig. 9. HOMO - LUMO plot of 3-2ADP.

Table 4. The calculated energy values of 3-2ADP.

Parameters	Values
E_{LUMO}	-0.07 a.u
E_{HOMO}	-0.23 a.u
$E_{LUMO-HOMO}$ gap	4.23 eV
$I = - E_{HOMO}$	0.23 a.u
$A = - E_{LUMO}$	0.07 a.u
χ=I+A/2	0.15 a.u
η= I - A/2	0.07 a.u
S=1/2 η	0.03 $a.u^{-1}$
ω= χ2/2 η	9.28×10^{-4} $a.u^{-1}$

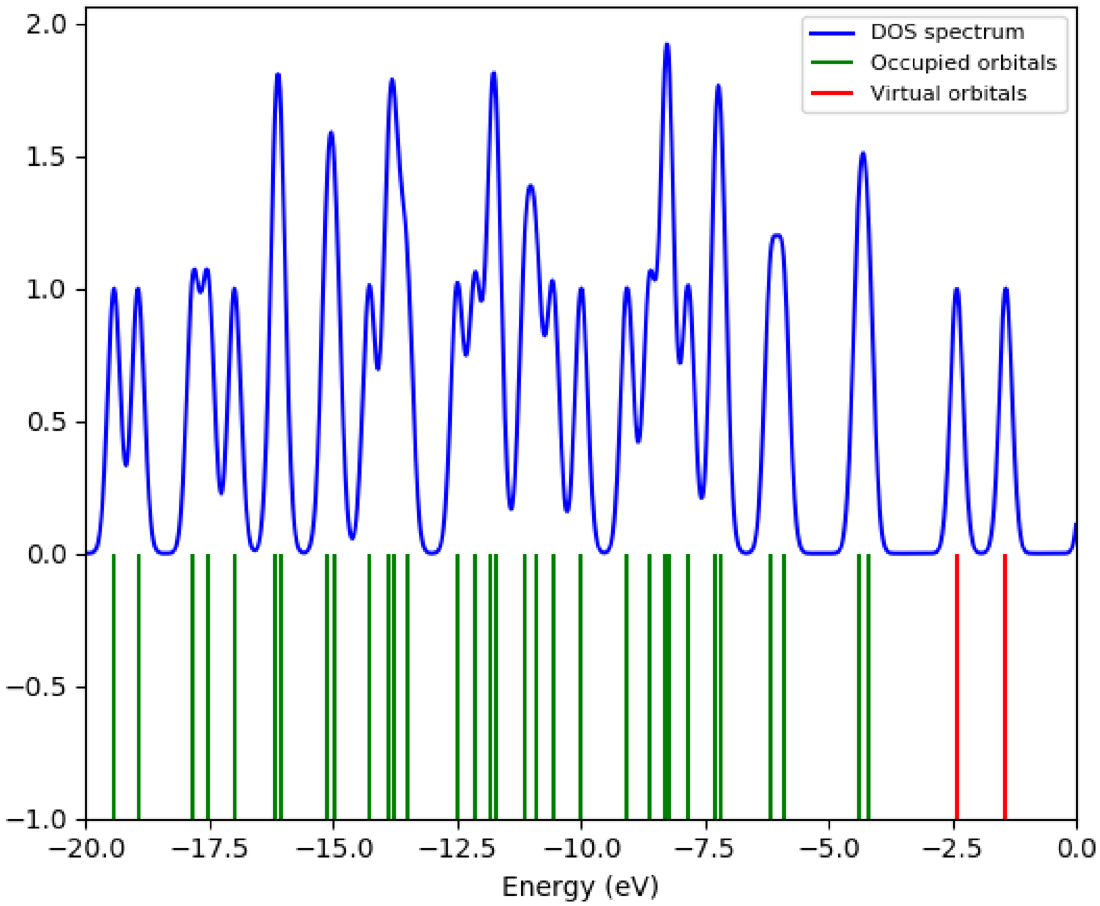

Fig. 10. Calculated the total DOS of 3-2ADP.

Molecular electrostatic potential

The electrostatic potential (ESP), the contour map of electrostatic potential and molecular electrostatic potential (MEP) plot of the 3-2ADP molecule obtained by Gaussian 03 package is illustrated in Fig. 11. It is most evident from the ESP map, that the negative electrostatic potential was concentrated over the entire 3-2ADP molecule. The contour map of the electrostatic potential confirmed the different positive and negative potential sides of the 3-2ADP compound. To predict reactive sites for electrophilic and nucleophilic attack for the 3-2ADP compound, MEP was computed at B3LYP/6-31 G(d, p) optimized geometries. MEP maps provide tridimensional load distribution of molecules and contribute to the correlation between the molecular structure and its physiochemical behavior such as partial loads, dipole moment, electronegativity and chemical reactivity [33]. Different colors reflect the different values of the electrostatic potential at the electron density surface. The molecule with red color represents regions of most electronegative and maximum attractive electrostatic potential whereas, blue color molecule represents regions of most positive and repulsive electrostatic potential and that of green represents the region of zero potential.

The result shows that MEP decreases in the order of red > orange > yellow > green > blue [34]. The different color code of these maps is in the range between -0.138e° (the dark red) and +0.138e° (the dark blue) for 3-2ADP molecule. This MEP surface provides significant information about the reactive sites of the molecules. The MEP map of 3-2ADP, the positive regions was found over the protonated amine group of 3-acetylanilinium moiety and the negative regions are spread over the electronegative oxygen atoms. Further, most of the C-atoms in the 3-2ADP molecule bear the green region

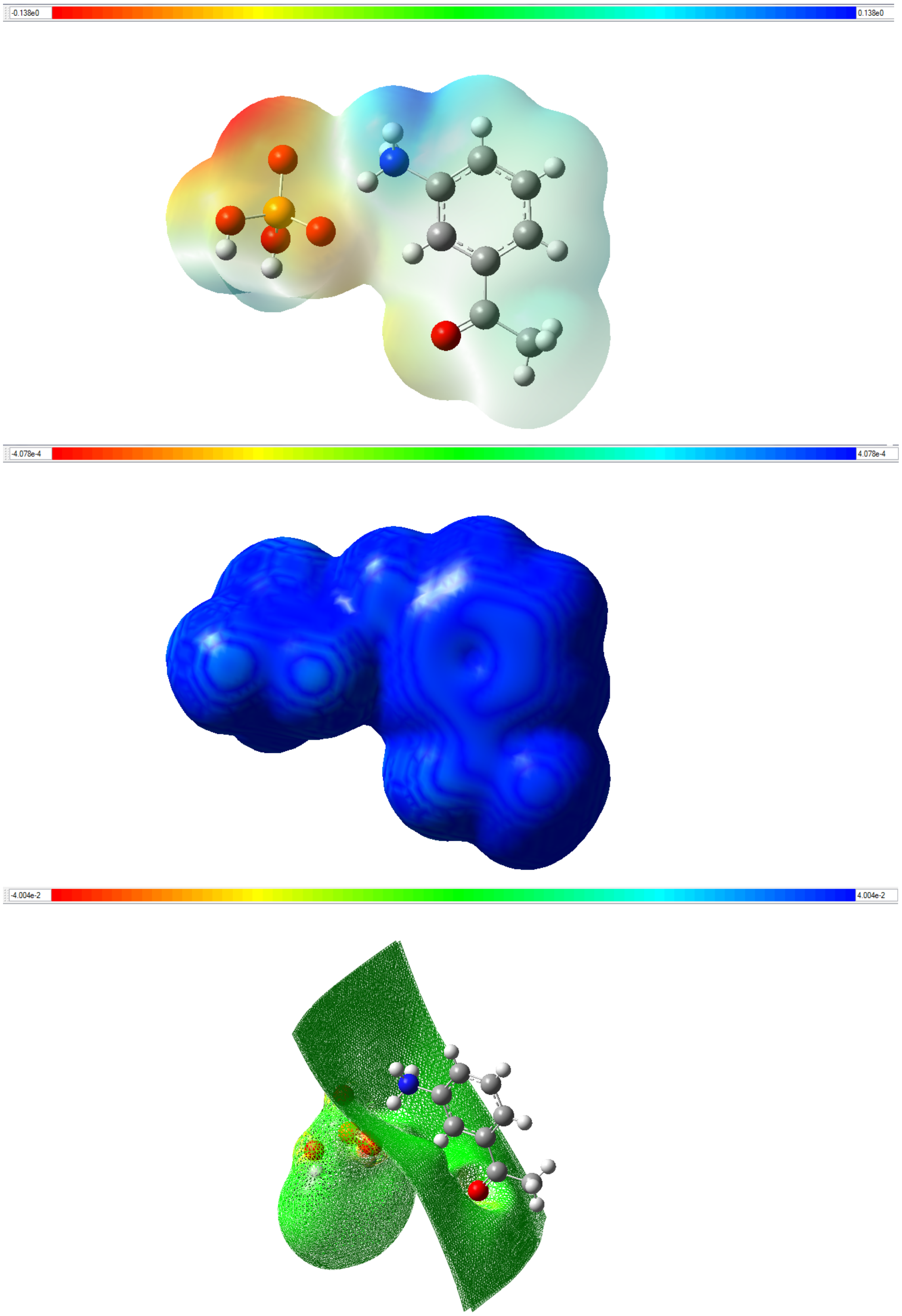

Fig. 11. The total electron density isosurface mapped with molecular electrostatic potential of 3-2ADP.

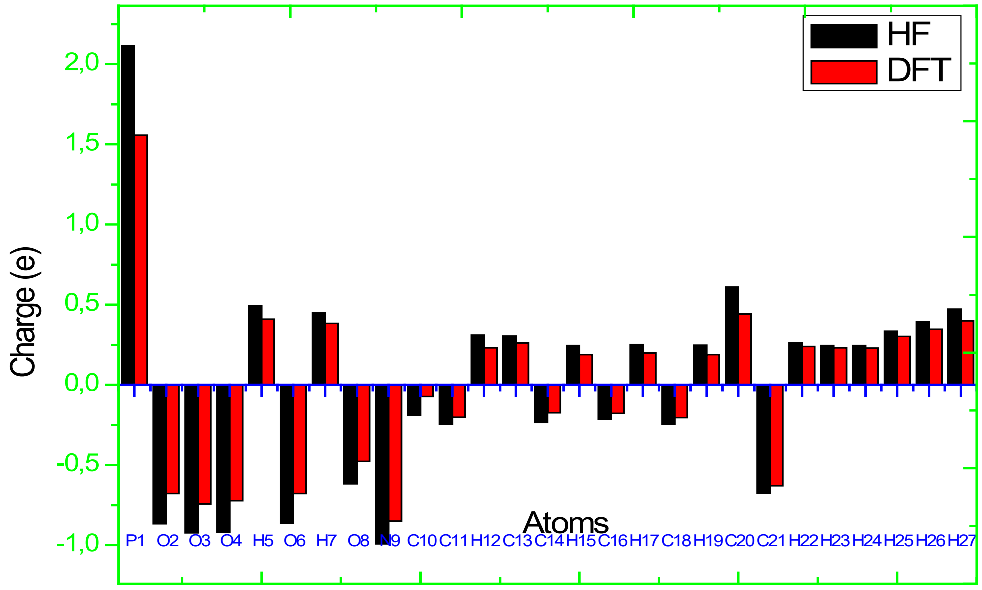

Fig. 12. Mulliken charges distribution of 3-2ADP.

in the MEP surfaces zero potential and it describes the potential halfway between the two extreme deepest red and blue colors. The inter- and intramolecular hydrogen bonding interactions such as N-H...O, C-H...O, and O-H...O of 3-acetylanilinium dihydrogen phosphate result from the equalization of molecular electrostatic potentials in the system (Fig. 11).

Mulliken and natural charge distribution

The Mulliken atomic charge distribution calculation is an important application of the quantum chemical approach to the molecular system by virtue of atomic charge effect, molecular polarizability, dipole moment, electronic structure and other characteristics of the molecular system [35, 36]. The Mulliken atomic charge distribution for 3-acetylanilinium dihydrogen phosphate is shown in Fig. 12, in Supplementary information and Mulliken plot of charge distribution for the titular compound, it is clearly noticed that the charge of amine atom N_9 of the 3-2ADP compound is highly negative and the corresponding protonated hydrogen H_{19} atoms have more positive charge compared to other hydrogen atoms. The charge of phosphate P-1 atom is positive it's surrounding four atoms oxygen O_2, O_3, O_4, and O_6 atoms have higher negative influence. In the aromatic ring, the negative values on C_{10}, C_{11}, C_{13}, C_{14}, C_{16}, and C_{18} atoms leads to the redistribution of electron density. As a result of these strong negative charges, C_{20} and C_{21} accommodate large positive charge and become more acidic. Further, it is also observed that the carbon atom C_{21} attains maximum positive charge due to its bonding with electronegative oxygen atom O_8. The total atomic charges of 3-2ADP crystal in the ground state obtained from DFT/B3LYP/6-31G (d, p) level (Fig. 12).

CONCLUSIONS

In summary, the phosphate $H_2PO_4^-$ ion with the $C_8H_{10}NO^+$ were investigated. A novel organic–inorganic hybid compound has been successfully synthesized at room temperature by slow evaporation in the DFT theoretically studied and Hirshfeld surfaces. The structure consists of alternating organic layers with inorganic ones. Hirshfeld surfaces show all intermolecular interactions in the crystal at once and are therefore suitable for crystal packing analysis. Global descriptors, such as the orbital energy gap (Eg), electronegativity (χ), absolute hardness (η), softness (σ), chemical potential (μ), electrophile index (ω) and Mulliken atomic charges were derived from the DFT and HF calculations.

REFERENCES

1. M.H. Jiang, Q. Fang, Organic and Semiorganic Nonlinear Optical Materials, Adv. Mater, 11, 1999, 1147-1151.
2. M.D. Aggarwal, J. Choi, W.S. Wang, K. Bhat, R.B. Lal, A.D. Shields, B.G. Penn, D.O. Frazier, Solution Growth of a Novel NLO Material: L-histidine tetrafluoroborate, J. Cryst. Growth, 204, 1999, 179-182.
3. J.C.E. Carraher, M.R. Roner, K. Shahi, G. Barot, Structural consideration in designing organotin polyethers to arrest the growth of breast cancer cells in vitro, Materials, 4, 2011, 801-815.
4. R. Masse, M. B. Beucher, J. Pecaut, J.P. Levy, J. Zyss, Design of organic–inorganic polar crystals for quadratic nonlinear optics, Nonlinear Opt, 5,1993, 413-423
5. C.R. Kagan, D.B. Mitzi, C.D. Dimitrakopoulos, Organic-inorganic hybrid materials as semiconducting channels in thin-film field-effect transistors, Science, 286, 1999, 945-947.
6. A. Rafik, H. Zouihri, T. Guedira, Hirshfeld surface analysis and quantum chemical study of molecular structure of phosphate, Bull. Chem. Soc. Ethiop, 35, 2021, 625-638.
7. D. Cincic, B. Kaitner, 3-Acetylanilinium bromide, nitrate and dihydrogen phosphate: hydrogen-bonding motifs in one, two and three dimensions, Acta Cryst, C64, 2008, 561-565.
8. G.C. Xiao, A new inorganic-organic hybrid based on biisoquinoline and hexachloridostannate: structure, photoluminescence, electrochemical behavior and theoretical study, Chin. J. Struct. Chem, 33, 2014, 1689-1696.
9. E.D. D'silva, G. Krishna Podagatlapalli, S. Venugopal Rao, S.M. Dharmaprakash, Structural, optical and electrical characteristics of a new NLO Crystal, Opt. Laser Techno, 44, 2012, 1689-1697.
10. M.R. Kumar, A. Chandramohan, synthesis, growth, characterisation and laser damage threshold studies of N,N-dimethylanilinium-3-carboxy-4-hydroxy benzene sulphonate crystal; An efficient SHG material for electro-optic applications, Opt. Mat, 66, 2017, 261-270.
11. P. Vivek, A. Suvitha, P. Murugakoothan, Growth, spectral, anisotropic, second and third order nonlinear optical studies on potential nonlinear optical crystal anilinium perchlorate (AP) for NLO device fabrications, Spectrochim. Acta Part A, 134, 2015, 517-525.
12. P. Nagapandiselvi, C. Baby, R. Gopalakrishnan, Synthesis, Growth, Structure and Nonlinear Optical Properties of a Semiorganic 2-Carboxypyridinium dihydrogen phosphate Single Crystal, Opt. Mater, 47, 2015, 398-405.
13. D.R. Babu, H. Arul, R. Ezhil Vizhi, Growth and Characterization of Morpholinium dihydrogenphosphate Single crystal, J. Cryst. Growth, 452, 2016, 220-225.
14. S.K. Wolff, D.J. Grimwood, J.J. McKinnon, M. J. Turner, D. Jayatilaka, M. A. Spackman, CrystalExplorer. University of Western Australia, 2012.
15. D. Jayatilaka, D.J. Grimwood, A. Lee, A. Lemay, A.J. Russel, C. Taylor, S. K. Wolff, P. Cassam-Chenai, & A. Whitton, TONTO, 2005, http://hirshfeldsurface.net/.
16. M.A. Spackman, J.J. McKinnon, D. Jayatilaka, CrystEngComm, 10, 2008, 377-388.
17. J.K. Labanowski, J. W. Andzelm, Density Functional Methods in Chemistry, New York: Springer Verlag, 1991.
18. C. Lee, W. Yang, R.G. Parr, Development of the Colle-Salvetti correlation-energy formula into a functional of the electron density, Phys Rev B, 37, 1988, 785-789.
19. M.J. Frisch, G.W. Trucks, H.B. Schlegel, G.E. Scuseria, M.A. Robb, J.R. Cheeseman, G.Scalmani, V. Barone, B. Mennucci, G.A. Petersson, H. Nakatsuji, M. Carinate, X. Li, H.P. Hratchian, A.F. Izmaylov, J. Bloino, G. Zheng, J.L. Sonnenberg, M. Hada, M. Ehara, K. Toyota, R. Fukuda, J. Hasegawa, M. Ishida, T. Nakajima, Y. Honda, O. Kitao, H. Nakai, T. Vreven, J.A. Montgomery, J.J. E. Peralta, F. Ogliaro, M. Bearpark, J.J. Heyd, E. Brothers, K. N. Kudin, V.N. Staroverov, R. Kobayashi, J. Normand, K. Raghavachari, A. Rendell, J.C. Burant, S.S. Iyengar, J. Tomasi, M. Cossi, N. Rega, J.M. Millam, M. Klene, J.E. Knox, J.B. Cross, V. Bakken, C. Adamo, J. Jaramillo, R. Gomperts, R.E. Stratmann, O. Yazyev, A.J. Austin, R. Cammi, C. Pomelli, J.W. Ochterski, R.L. Martin, K. Morokuma, V.G. Zakrzewski, G.A. Voth, P. Salvador, J.J. Dannenberg,

S. Dapprich, A.D. Daniels, O.Farkas, J.B. Foresman, J. V. Ortiz, J. Cioslowski, D.J. Fox, Gaussian 09 (Revision D.01), Gaussian Inc, Wallingford, CT, 2009.

20. M.J. Turner, J.J. MacKinnon, S.K. Wolff, D.J. Grimwood, P.R. Spackman, D. Jayatilaka, & M.A. Spackman, CrystalExplorer17.5. University of Western Australia, 2017, http://hirshfeldsurface.net
21. H. Saeidian, M. Sahandi, Comprehensive DFT study on molecular structures of lewisites in support of the chemical weapons convention, J. Mol. Struct, 1100, 2015, 486-495.
22. H. Gokçe, S. Bahçeli, FT-IR, micro-Raman and UV-Vis spectroscopic and quantum chemical investigations of free 2, 20-dithiodipyridine and its metal (Co, Cu and Zn) halide complexes, Spectrochim. Acta A, 114, 2013, 61-73.
23. W. Kohn, A.D. Becke, R.G. Parr, Density functional theory of electronic structure, J. Phys. Chem, 100, 1996, 12974-12980.
24. L. Xiao-Hong, L. Xiang-Ru, Z. Xian-Zhou, Molecular structure and vibrational spectra of three substituted 4-thioflavones by density functional theory and ab initio HartreeeFock calculations, Spectrochim, Acta Part A, 78, 2011, 528-536.
25. S. Muthu, E.I. Paulraj, Spectroscopic and molecular structure (monomeric and dimeric structure) investigation of 2-[(2hydroxyphenyl) carbonyloxy] benzoic acid by DFT method: a combined experimental and theoretical study, J. Mol. Struct, 1038, 2013, 145-162.
26. K. Sambathkumar, S. Jeyavijayan, M. Arivazhagan, Electronic structure investigations of 4-aminophthal hydrazide by UV–visible, NMR spectral studies and HOMO–LUMO analysis by ab initio and DFT calculations, Spectrochim. Acta A, 147, 2015, 124-138.
27. H. Moghanian, A. Mobinikhaledi, R. Monjezi, Synthesis, spectroscopy (vibrational, NMR and UV-vis) studies, HOMO-LUMO and NBO analysis of 8-formyl-7-hydroxy- 4-methylcoumarin by ab initio calculations. J. Mol. Struct, 1052, 2013, 135-145.
28. E. Reed, L. A. Curtiss, F. Weinhold, Intermolecular interactions from a natural bond orbital, donor-acceptor viewpoint, Chem. Rev, 88, 1988, 899-926.
29. Ravikumar, I.H. Joe, V. Jayakumar, Charge transfer interactions andnonlinear optical properties of push pull chromophore benzaldehyde phenylhydrazone: a vibrational approach, Chem. Phys. Lett., 460, 2008, 552-558.
30. J. C. Cramer, Essentials of the Computational Chemistry: Theories and Models, second ed., 14, John Wiley and Sons Ltd., West Suss, 6, 2007, 578-501.
31. R.I. Al-Wabli, A. Salman, V. Shyni, H.A. Ghabbour, I.H. Joe, M.S. Almutairi, Y.A. Maklad, M.I. Attia, Synthesis, crystal structure, vibrational profiling, DFT studies and molecular docking of N-(4-chloro-2-{[2-(1H-indol-2-ylcarbonyl) hydrazinyl] (oxo) acetyl}phenyl) acetamide. DMSO: a new antiproliferative agent, J. Mol. Struct., 1155, 2018, 457-468.
32. J. Chocholousova, V. Spirko, P. Hobza, First local minimum of the formic acid dimer exhibits simultaneously red-shifted O-H…O and improper blue shifted C-H…O hydrogen bonds, Phys. Chem. Chem. Phys., 6, 2004, 37-41.
33. K. Sarojini, H. Krishnan, C.C. Kanagam, S. Muthu, Molecular structure, vibrational spectroscopy and Homo, Lumo studies of 4-methyl-N-(2-methylphenyl) benzene sulfonamide using DFT method, Adv. Mater. Res., 665, 2013, 101-111.
34. V. Balachandran, A. Lakshmi, A. Janaki, Conformational stability, vibrational spectral studies, HOMO-LUMO and NBO analyses of 2-hydroxy-4-methyl-3-nitropyridine and 2-hydroxy-4-methyl-5 nitropyridine based on density functional theory, J. Mol. Struct., 1013, 2012, 75-85.
35. S. Gunasekaran, S. Kumaresan, R. Arunbalaji, G. Anand, S. Srinivasan, Density functional theory study of vibrational spectra, and assignment of fundamental modes of dacarbazine, J. Chem. Sci., 120, 2008, 315-324.
36. A. Esme, S.G. Sagdinc, The vibrational studies and theoretical investigation of structure, electronic and non-linear optical properties of Sudan III [1-{[4-(phenylazo) phenyl]azo}- 2-naphthalenol], J. Mol. Struct., 1048, 2013, 185-195.